

# Self-Host Blue-Emitting Iridium Dendrimer with Carbazole Dendrons: Nondoped Phosphorescent Organic Light-Emitting Diodes\*\*

Debin Xia, Bin Wang, Bo Chen, Shumeng Wang, Baohua Zhang, Junqiao Ding,\*  
Lixiang Wang,\* Xiabin Jing, and Fosong Wang

**Abstract:** A blue-emitting iridium dendrimer, namely **B-G2**, has been successfully designed and synthesized with a second-generation oligocarbazole as the dendron, which is covalently attached to the emissive tris[2-(2,4-difluorophenyl)pyridyl]iridium(III) core through a nonconjugated link to form an efficient self-host system in one dendrimer. Unlike small molecular phosphors and other phosphorescent dendrimers, **B-G2** shows a continuous enhancement in the device efficiency with increasing doping concentration. When using neat **B-G2** as the emitting layer, the nondoped device is achieved without loss in efficiency, thus giving a state-of-art EQE as high as 15.3 % ( $31.3 \text{ cd A}^{-1}$ ,  $28.9 \text{ lm W}^{-1}$ ) along with CIE coordinates of (0.16, 0.29).

The exploration of suitable phosphors for nondoped phosphorescent organic light-emitting diodes (PhOLEDs),<sup>[1]</sup> which can be used alone as the emitting layer (EML) without the need to be dispersed into an additional host matrix, has become an increasingly exciting area of research. Compared with conventional doped PhOLEDs,<sup>[2]</sup> the careful work on precise control over the doping content of phosphors and inevitable phase segregation<sup>[3]</sup> are both avoided to simplify the device fabrication process, and improve device stability and reproducibility. Most importantly, this nondoped technology seems especially attractive for blue emission since the appropriate hosts, having large band gaps for blue emitters, are still mostly elusive.<sup>[4]</sup> There is therefore a need to develop host-free blue-emitting phosphors.

Phosphorescent dendrimers present one pathway toward this end.<sup>[5]</sup> With a triplet emitter located at the central core, the strong interactions between emissive cores can be well

modulated to reduce or eliminate the quenching of the luminance by the site isolation effect.<sup>[6]</sup> Early in 2005, P. L. Burn et al. firstly reported blue iridium (Ir) dendrimers with biphenyl dendrons, and fabricated their corresponding nondoped PhOLEDs, but there was a loss in device performance with an external quantum efficiency (EQE) of 3.8 %.<sup>[7]</sup> It was further improved to 7.9 % by using a different triplet core in 2008.<sup>[8]</sup> Since then little progress has been made because of the scarcity of functional dendrons with high triplet energy and good charge transport.<sup>[9]</sup>

Herein, we report the blue Ir dendrimer **B-G2**, having a radius of 23 Å, which can be used for the fabrication of high-performance nondoped PhOLEDs. As illustrated in Figure 1,

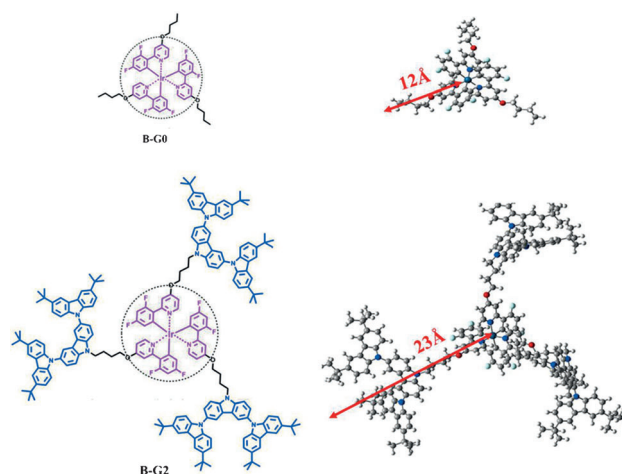


**Figure 1.** The designed self-host blue-emitting iridium dendrimer **B-G2** and model compound **B-G0**.

tris[2-(2,4-difluorophenyl)pyridyl]iridium(III) [Ir(dfppy)<sub>3</sub>] is employed as the triplet core owing to the intense room-temperature blue phosphorescence.<sup>[10]</sup> Meanwhile, the second-generation oligocarbazole is selected as the dendron because the carbazole unit possesses a triplet energy of about 3.0 eV, as well as an excellent hole-transporting capability, and has been widely applied as the building block for the design of wide-band-gap host materials and multifunctional phosphors.<sup>[11]</sup> In addition, an ether linkage is incorporated between the core and dendron for convenient synthesis while simultaneously not altering the core's emission. Here the four-carbon-atom chain is preferentially utilized because the carbazole-containing alkyl bromide with shorter chains is unstable, and thus undergoes elimination reactions and forms inactive olefins.<sup>[12]</sup> Although the chain-length of the spacer

[\*] D. Xia,<sup>[†]</sup> B. Wang,<sup>[†]</sup> B. Chen, S. Wang, Dr. B. Zhang, Dr. J. Ding, Prof. L. Wang, Prof. X. Jing, Prof. F. Wang  
State Key Laboratory of Polymer Physics and Chemistry, Changchun Institute of Applied Chemistry, Chinese Academy of Sciences  
Changchun 130022 (P. R. China)  
E-mail: junqiaod@ciac.ac.cn  
lixiang@ciac.ac.cn

B. Chen, S. Wang  
University of the Chinese Academy of Sciences  
Beijing 100049 (P. R. China)

[†] These authors contributed equally to this work.

[\*\*] We are grateful to the 973 Project (2009CB623601 and 2009CB930603), National Natural Science Foundation of China (Nos. 20923003, 21174144 and 21074130), and Science Fund for Creative Research Groups (No. 20921061) for financial support of this research.

Supporting information for this article is available on the WWW under <http://dx.doi.org/10.1002/ange.201307311>.

**Table 1:** The photophysical, electrochemical, and thermal properties of the dendrimers.

	$\lambda_{\text{abs}}$ (log $\epsilon$ ) <sup>[a]</sup> [nm]	$\lambda_{\text{s}}$ <sup>[b]</sup> [nm]	$\lambda_{\text{f}}$ <sup>[c]</sup> [nm]	$\Phi_{\text{PL}}$ <sup>[b]</sup>	$E_{\text{g}}$ <sup>[d]</sup> [eV]	$\tau_{\text{av}}$ <sup>[e]</sup> [ $\mu\text{s}$ ]	HOMO <sup>[f]</sup> [eV]	LUMO <sup>[f]</sup> [eV]	$T_{\text{g}}/T_{\text{d}}$ [°C]
<b>B-G0</b>	236 (4.8), 264 (4.8), 320 (4.0), 348 (4.1), 381 (3.9), 419 (3.4), 447 (2.9)	467	484	0.57	2.69	0.11	−5.23	−2.54	n.d./355
<b>B-G2</b>	241 (5.7), 268 (5.4), 297 (5.3), 335 (4.8), 350 (4.7), 381 (4.1), 420 (3.5), 442 (3.3)	467	468	0.69	2.68	0.59	−5.26	−2.58	271/437

[a] Measured in  $10^{-5}$  M dichloromethane solution. [b] Measured in  $\text{N}_2$ -saturated toluene solution with a concentration of  $10^{-5}$  M, and  $[\text{Ir}(\text{ppy})_3]$  ( $\Phi_{\text{PL}}=0.40$ ) is used as the reference. [c] Measured in neat films. [d] The optical band gap estimated from the absorption onset. [e] Measured in neat films under  $\text{N}_2$  excited at  $\lambda=355$  nm. [f] HOMO =  $-e(E_{\text{ox}}^{\text{onset}} + 4.8 \text{ V})$ , LUMO = HOMO +  $E_{\text{g}}$ .

may have some influence on device performance and further experiments should be performed, they are beyond the scope of this work.

With this design strategy, an efficient self-host system was formed in one dendritic molecule (**B-G2**), where the surrounding carbazole dendrons are expected to function as the host for the emissive core. Therefore, unlike small molecular phosphors and other phosphorescent dendrimers known to date, the nondoped **B-G2** device has been achieved without the expense of efficiency for the first time, thus generating a state-of-art EQE as high as 15.3% ( $31.3 \text{ cd A}^{-1}$ ,  $28.9 \text{ lm W}^{-1}$ ) along with Commission Internationale de l'Eclairage (CIE) coordinates of (0.16, 0.29).

The synthesis of **B-G2** is depicted in Scheme S1 of the Supporting Information). *n*-Butyl bromide terminated second-generation carbazole dendron underwent a nucleophilic substitution to afford the ether-linked product in a high yield (69%), and was then reacted with 2,4-difluorophenylboronic acid by Suzuki–Miyaura cross-coupling to give the target dendritic ligand. Finally, given the poor solubility of dendritic ligand in glycerol, a modified two-step procedure was adopted to synthesize **B-G2**. That is, a  $\mu$ -chloride-bridged dimer was initially formed, followed by the further ligation with the dendritic ligand in mesitylene and catalyzed by  $\text{AgSO}_3\text{CF}_3$ . Under these reaction conditions, the facial isomer was directly obtained and isolated in an acceptable total yield of 26%, which was confirmed by the  $^1\text{H}$  NMR spectrum of **B-G2** (see Figure S4 in the Supporting Information) showing only one set of ligand signals.<sup>[11]</sup> As a prototype, **B-G0**, without dendrons was also prepared to reveal the self-host nature of **B-G2**.

Thermogravimetric analysis (TGA) and differential scanning calorimetry (DSC) were used to examine the thermal properties of **B-G2**. It is thermally stable with a high decomposition temperature ( $T_{\text{d}}$ : at a 5% weight loss) of 437°C. Furthermore, even in the presence of flexible alkoxy units, **B-G2** displays an unexpected glass-transition temperature ( $T_{\text{g}}$ ) as high as 271°C, which is far superior to those of biphenyl-based blue Ir dendrimers (70–150°C).<sup>[7–8,9a]</sup> The enhanced  $T_{\text{g}}$  of **B-G2** might arise from a higher degree of dendron rigidity derived from carbazole relative to that of biphenyl, and it is highly desirable to attain effective encapsulation for the Ir core.

The photophysical properties of **B-G0** and **B-G2** were firstly explored, and the corresponding data are summarized in Table 1. As depicted in Figure S9 (see the Supporting Information), **B-G2** has intense absorption bands below  $\lambda=$

300 nm, which are assigned to the spin-allowed ligand-centered (LC) transitions, and weaker metal-to-ligand charge-transfer (MLCT) transitions in the  $\lambda=300$ –450 nm region. With respect to **B-G0**, the intensity of the absorption at around  $\lambda=240$  nm, characteristic of the carbazole moiety in **B-G2**, is found to be strengthened after the introduction of oligocarbazole. The photoluminescent (PL) spectra of **B-G2** and **B-G0** both in toluene and in the solid state are shown in Figure 2. Both **B-G0** and **B-G2** exhibit the same emission maxima at  $\lambda=467$  nm with an identical spectral profile in toluene solutions, similar to that of the  $[\text{Ir}(\text{dfppy})_3]$  core.<sup>[10]</sup>

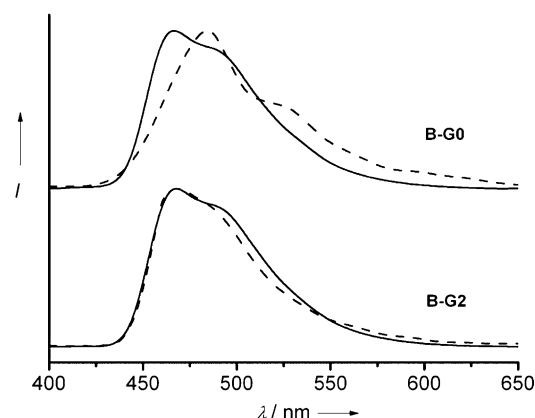


**Figure 2.** The PL spectra in toluene (solid lines) and neat film (dashed lines) of **B-G0** and **B-G2**.

This similarity is reasonable since the carbazole dendrons are linked to the emissive core through a nonconjugated spacer.

In neat films, however, different PL behaviors are observed for **B-G0** and **B-G2**. On going from solution to the solid state, **B-G0** shows a bathochromic shift of about 17 nm, which is associated with the appearance of a long tail in the range of  $\lambda=520$ –650 nm, and indicative of the existence of strong intermolecular interactions for **B-G0**. Unlike **B-G0**, the PL spectrum of **B-G2** (film) matches well with that in solution, thus suggesting that the interactions between emissive Ir cores in **B-G2** are almost completely suppressed by the attached carbazole dendrons. This feature is further verified by the film transient PL spectra of **B-G0** and **B-G2**. As can be clearly seen in Figure S10 in the Supporting Information, **B-G2** decays much more slowly than **B-G0**. Accordingly, the average lifetime, estimated by a biexponential fit of emission decay curves, increases from 0.11  $\mu\text{s}$  for **B-**

**G0** to 0.59  $\mu\text{s}$  for **B-G2** (Table 1 and S1 in the Supporting Information).

Their electrochemical properties were also investigated by cyclic voltammetry (CV) with the ferrocene/ferrocenium ( $\text{Fc}/\text{Fc}^+$ ) couple as the reference. During the anodic sweeping in dichloromethane, multiple oxidation waves were observed for **B-G2**. Based on the CV curve of **B-G0**, the first *p*-doping process in **B-G2** can be ascribed to one-electron oxidation of the Ir-phenyl center, while the others located at more positive potentials are related to the surrounding carbazole dendrons (see Figure S11 in the Supporting Information). The corresponding HOMO level of **B-G2** is determined to be  $-5.26\text{ eV}$ , close to that of **B-G0**. According to the optical band gap ( $E_g$ ) estimated from the absorption onset, the LUMO levels of **B-G0** and **B-G2** are calculated to be  $-2.54$  and  $-2.58\text{ eV}$ , respectively. The similar energy-level alignment of **B-G2** and **B-G0** further illustrates that the nonconjugated linkage is beneficial to maintain the properties of the emissive Ir core.

PhOLEDs of **B-G2** were fabricated with a configuration of ITO/PEDOT:PSS (40 nm)/**H2:B-G2** (40 nm)/SPPO13 (50 nm)/LiF (1 nm)/Al (100 nm), where **H2** and SPPO13 (2,7-bis(diphenylphosphoryl)-9,9'-spirobifluorene) acted as the host and electron-transporting materials, respectively (see Figure S12 in the Supporting Information).<sup>[11a,13]</sup> For comparison, devices with **H2:B-G0** as the EML were also prepared under the same conditions. The ratio of **B-G2** in **H2** was firstly tuned to evaluate its potential as a host-free phosphor. As presented in Figure 3, the luminous efficiency continuously increases with the increasing doping content, and reaches the maximum value when **B-G2** is used in its undiluted form. As a result, unlike **B-G0**, whose best device performance is obtained at a low-doping concentration of 20 wt%, the nondoped device efficiency of **B-G2** is significantly higher than those of corresponding doped devices. To the best of our knowledge, this is the first report that nondoped PhOLEDs are realized without sacrificing the efficiency. In this respect, **B-G2** differs from blue Ir dendrimers with biphenyl dendrons.<sup>[7–8,9a]</sup> Furthermore, it should be noted that the interesting doping concentration dependence of **B-G2** is also quite different from that previously reported for green- and red-emitting Ir dendrimers,<sup>[14]</sup> even if the same size carbazole dendron is used to encapsulate the Ir core. The reason lies in that, apart from the carbazole dendron, the F substituents in **B-G2** may also contribute to modifying the molecular packing and thereby minimizing the self-quenching behavior.<sup>[15]</sup>

Figure S13 in the Supporting Information compares the electroluminescent (EL) spectra between the nondoped devices of **B-G0** and **B-G2**. Noticeably, the EL spectrum of **B-G2** is nearly identical to its PL counterpart, thus showing blue triplet emission with CIE coordinates of (0.16, 0.29). In contrast, the  $\lambda = 490\text{ nm}$  emission related to 0–1 transition dominates the whole EL spectrum of **B-G0**, thus leading to red-shifted CIE coordinates of (0.18, 0.32). Consistent with the difference between the film PL spectra of **B-G0** and **B-G2** as discussed above, these observations indicate that there exists severe aggregation-induced self-

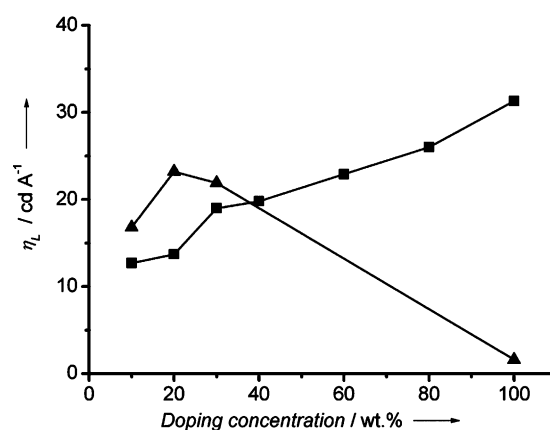


**Figure 3.** The doping concentration dependence of the luminous efficiency ( $\eta_L$ ) for **B-G0**- (▲) and **B-G2**-based (■) PhOLEDs.

quenching in **B-G0**, whereas this quenching turns out to be negligible in **B-G2** because of the shielding effect from periphery dendrons.

It is thus understandable that, the peak luminous efficiency, power efficiency, and EQE are prominently enhanced from  $1.6\text{ cd A}^{-1}$ ,  $1.2\text{ lm W}^{-1}$ , and 0.7% for **B-G0** to  $31.3\text{ cd A}^{-1}$ ,  $28.9\text{ lm W}^{-1}$ , and 15.3% for **B-G2**, respectively (Table 2). The resulting EQE for **B-G2** is about 22-fold that of the nondoped device of **B-G0**. And this value is even 29% higher than that of the optimized doped device **H2:B-G0** (20 wt.%), which reveals an EQE of  $11.9\%$  ( $23.2\text{ cd A}^{-1}$ ,  $18.2\text{ lm W}^{-1}$ ; Figure 4b). Together with the fact that there is

**Table 2:** Summary of electroluminescence data for PhOLEDs.

EML	$V_{\text{on}}^{[a]}$ [V]	Brightness <sup>[b]</sup> [ $\text{cd m}^{-2}$ ]	$\eta_L^{[b]}$ [ $\text{cd A}^{-1}$ ]	$\eta_p^{[b]}$ [ $\text{lm W}^{-1}$ ]	EQE <sup>[b]</sup> [%]	CIE <sup>[c]</sup> [x, y]
<b>H2:B-G0</b> (10 wt %)	3.5	4940	16.8	14.4	7.8	(0.16, 0.32)
<b>H2:B-G0</b> (20 wt %)	3.6	6050	23.2	18.2	11.9	(0.15, 0.26)
<b>H2:B-G0</b> (30 wt %)	3.4	6700	21.8	20.0	10.9	(0.16, 0.27)
<b>B-G0</b> (100 wt %)	3.2	1140	1.6	1.2	0.7	(0.18, 0.32)
<b>H2:B-G2</b> (10 wt %)	4.2	2940	11.4	7.2	5.8	(0.16, 0.29)
<b>H2:B-G2</b> (20 wt %)	3.7	3720	13.8	10.7	7.0	(0.15, 0.23)
<b>H2:B-G2</b> (30 wt %)	3.5	4420	19.0	15.6	10.1	(0.15, 0.26)
<b>H2:B-G2</b> (40 wt %)	3.1	5190	19.8	17.0	9.7	(0.15, 0.29)
<b>H2:B-G2</b> (60 wt %)	3.2	6160	23.0	19.4	11.2	(0.15, 0.29)
<b>H2:B-G2</b> (80 wt %)	3.2	6530	26.8	23.3	13.1	(0.15, 0.29)
<b>B-G2</b> (100 wt %)	3.6	6800	31.3	28.9	15.3	(0.16, 0.29)

[a] Turn-on voltage at a brightness of  $1\text{ cd m}^{-2}$ . [b] The maximum data for brightness, luminous efficiency ( $\eta_L$ ), power efficiency ( $\eta_p$ ), and external quantum efficiency (EQE). [c] CIE at 7 V.

no phase separation, no tedious work on the control of doping ratios, and no requirement for wide-band-gap hosts in this case, the efficiency improvement powerfully demonstrates the advantage of a self-host system over a physical blend. Additionally, in Figure 4a, we note that the maximum brightness of **B-G2** is comparable to that of **H2:B-G0** (20 wt.%), which may be attributed to the two favorable charge-transport routes in a neat **B-G2** EML. On one hand, the effective charge injection distance into the Ir core is below

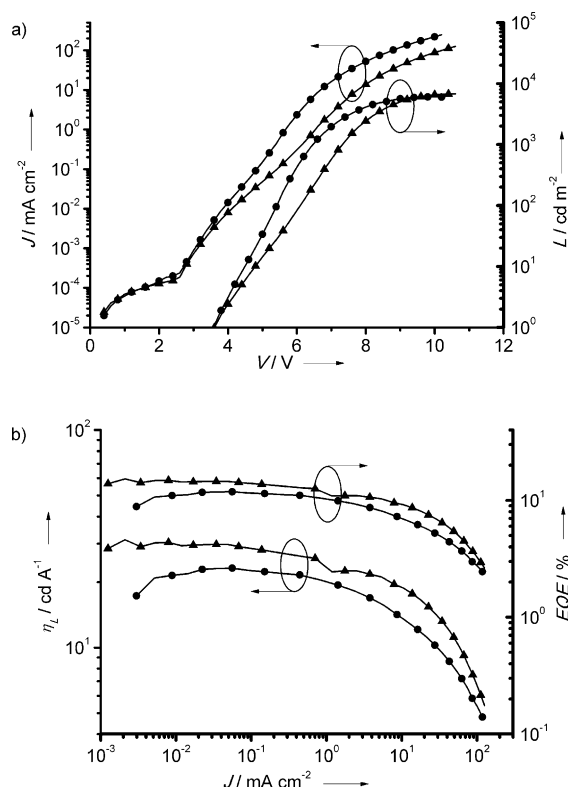


**Figure 4.** The current density-voltage-luminance ( $J$ - $V$ - $L$ ) characteristics (a) and luminous efficiency ( $\eta_L$ ) and EQE as a function of current density ( $J$ ) (b) for the nondoped **B-G2** ( $\blacktriangle$ ) and optimized doped device of **H2:B-G0** (20 wt%;  $\bullet$ ).

30 Å according to the literature.<sup>[16]</sup> Therefore, intramolecular charge transport can happen from the carbazole dendron to the core because **B-G2** has a moderate molecular size of 23 Å. On the other hand, the presence of the carbazole dendron can facilitate intermolecular charge transport between neighboring dendrons. Through these two processes, excitons can be directly generated on the Ir core, or firstly formed on carbazole dendron and then transferred to the core, thus resulting in bright luminance for the **B-G2**-based nondoped device.

As listed in Table 2, a maximum luminous efficiency of 31.3 cd A<sup>-1</sup>, a maximum power efficiency of 28.9 lm W<sup>-1</sup>, a peak EQE of 15.3%, and a maximum brightness of 6800 cd m<sup>-2</sup> have been achieved for the nondoped device of **B-G2**. The comprehensive performance is the best among reported blue Ir dendrimers.<sup>[7–8,9a]</sup> Compared with biphenyl-based dendrimers (3.8%), the EQE of **B-G2** is enhanced by about four times.<sup>[7]</sup> Taking into account that the emissive core is the same, the improvement can be ascribed to the incorporation of carbazole dendrons: 1) the electron-rich nature of carbazole endows **B-G2** with good hole-transport property; 2) the triplet energy of carbazole dendron is higher than that of the biphenyl dendron, thus avoiding the loss of triplet excitons;<sup>[17]</sup> and 3) the more effective encapsulation could be envisioned to control the intermolecular interactions in **B-G2** because of the aforementioned better rigidity of carbazole dendron in comparison to biphenyl dendron.

In conclusion, we have demonstrated that an efficient self-host system can be successfully constructed in blue Ir dendrimers on the basis of the second-generation carbazole dendron. The designed dendrimer **B-G2** has a different doping concentration dependence from both small molecular phosphors and other phosphorescent dendrimers, and exhibits a promising nondoped device EQE of 15.3% (31.3 cd A<sup>-1</sup>, 28.9 lm W<sup>-1</sup>). As **B-G2** represents the first example whose nondoped device performance outperforms the corresponding doped devices, we believe that this work will shed light on the development of self-host phosphorescent dendrimers for applications in nondoped PhOLEDs.

Received: August 20, 2013

Revised: September 24, 2013

Published online: December 6, 2013

**Keywords:** dendrimers · heterocycles · iridium · supramolecular chemistry · synthesis design

- [1] a) J. Li, D. Liu, *J. Mater. Chem.* **2009**, *19*, 7584; b) H. Jiang, *Macromol. Rapid Commun.* **2010**, *31*, 2007.
- [2] a) M. A. Baldo, D. F. O'Brien, Y. You, A. Shoustikov, S. Sibley, M. E. Thompson, S. R. Forrest, *Nature* **1998**, *395*, 151; b) M. A. Baldo, S. Lamansky, P. E. Burrows, M. E. Thompson, S. R. Forrest, *Appl. Phys. Lett.* **1999**, *75*, 4.
- [3] a) F. C. Chen, S. C. Chang, G. F. He, S. Pyo, Y. Yang, M. Kurotaki, J. Kido, *J. Polym. Sci. Part B* **2003**, *41*, 2681; b) F. C. Chen, G. F. He, Y. Yang, *Appl. Phys. Lett.* **2003**, *82*, 1006; c) Y. Y. Noh, C. L. Lee, J. J. Kim, K. Yase, *J. Chem. Phys.* **2003**, *118*, 2853.
- [4] a) K. Brunner, A. van Dijken, H. Börner, J. Bastiaansen, N. M. M. Kiggen, B. M. W. Langeveld, *J. Am. Chem. Soc.* **2004**, *126*, 6035; b) A. van Dijken, J. Bastiaansen, N. M. M. Kiggen, B. M. W. Langeveld, C. Rothe, A. Monkman, I. Bach, P. Stossel, K. Brunner, *J. Am. Chem. Soc.* **2004**, *126*, 7718; c) S. Shao, J. Ding, L. Wang, X. Jing, F. Wang, *J. Am. Chem. Soc.* **2012**, *134*, 15189; d) S. Shao, J. Ding, L. Wang, X. Jing, F. Wang, *J. Am. Chem. Soc.* **2012**, *134*, 20290; e) C.-L. Ho, W.-Y. Wong, *New J. Chem.* **2013**, *37*, 1665.
- [5] a) S.-H. Hwang, C. N. Moorefield, G. R. Newkome, *Chem. Soc. Rev.* **2008**, *37*, 2543; b) A. C. Grimsdale, K. L. Chan, R. E. Martin, P. G. Jokisz, A. B. Holmes, *Chem. Rev.* **2009**, *109*, 897; c) W.-Y. Wong, C.-L. Ho, *Coord. Chem. Rev.* **2009**, *253*, 1709; d) C. Zhong, C. Duan, F. Huang, H. Wu, Y. Cao, *Chem. Mater.* **2011**, *23*, 326; e) S.-C. Lo, P. L. Burn, *Chem. Rev.* **2007**, *107*, 1097; f) G. Zhou, W.-Y. Wong, X. Yang, *Chem. Asian J.* **2011**, *6*, 1706.
- [6] a) T. Weil, E. Reuther, K. Müllen, *Angew. Chem.* **2002**, *114*, 1980; *Angew. Chem. Int. Ed.* **2002**, *41*, 1900; b) G. R. Newkome, C. N. Moorefield, F. Vögtle, *Dendritic Molecules: Concept, Synthesis and Perspectives*, Wiley-VCH, Weinheim, **1996**.
- [7] S. C. Lo, G. J. Richards, J. P. J. Markham, E. B. Namdas, S. Sharma, P. L. Burn, I. D. W. Samuel, *Adv. Funct. Mater.* **2005**, *15*, 1451.
- [8] S.-C. Lo, R. N. Bera, R. E. Harding, P. L. Burn, I. D. W. Samuel, *Adv. Funct. Mater.* **2008**, *18*, 3080.
- [9] a) S.-C. Lo, R. E. Harding, C. P. Shipley, S. G. Stevenson, P. L. Burn, I. D. W. Samuel, *J. Am. Chem. Soc.* **2009**, *131*, 16681; b) G. Zhou, W.-Y. Wong, B. Yao, Z. Xie, L. Wang, *Angew. Chem.* **2007**, *119*, 1167; *Angew. Chem. Int. Ed.* **2007**, *46*, 1149.
- [10] A. B. Tamayo, B. D. Alleyne, P. I. Djurovich, S. Lamansky, I. Tsyba, N. N. Ho, R. Bau, M. E. Thompson, *J. Am. Chem. Soc.* **2003**, *125*, 7377.
- [11] a) J. Ding, B. Zhang, J. Lü, Z. Xie, L. Wang, X. Jing, F. Wang, *Adv. Mater.* **2009**, *21*, 4983; b) K. S. Yook, J. Y. Lee, *Adv. Mater.*

- 2012**, 24, 3169; c) Y. Tao, C. Yang, J. Qin, *Chem. Soc. Rev.* **2011**, 40, 2943; d) W.-Y. Wong, C.-L. Ho, Z.-Q. Gao, B.-X. Mi, C.-H. Chen, K.-Y. Cheah, Z. Lin, *Angew. Chem.* **2006**, 118, 7964; *Angew. Chem. Int. Ed.* **2006**, 45, 7800; e) C.-L. Ho, Q. Wang, C.-S. Lam, W.-Y. Wong, D. Ma, L. Wang, Z.-Q. Wang, C.-H. Chen, K.-Y. Cheah, Z. Lin, *Chem. Asian J.* **2009**, 4, 89.
- [12] X. Li, J. Wang, R. Mason, X. R. Bu, J. Harrison, *Tetrahedron* **2002**, 58, 3747.
- [13] K. S. Yook, S. E. Jang, S. O. Jeon, J. Y. Lee, *Adv. Mater.* **2010**, 22, 4479.
- [14] a) J. Ding, J. Gao, Y. Cheng, Z. Xie, L. Wang, D. Ma, X. Jing, F. Wang, *Adv. Funct. Mater.* **2006**, 16, 575; b) J. Ding, J. Lü, Y. Cheng, Z. Xie, L. Wang, X. Jing, F. Wang, *Adv. Funct. Mater.* **2008**, 18, 2754; c) J. Ding, B. Wang, Z. Yue, B. Yao, Z. Xie, Y. Cheng, L. Wang, X. Jing, F. Wang, *Angew. Chem.* **2009**, 121, 6792; *Angew. Chem. Int. Ed.* **2009**, 48, 6664.
- [15] Y. Wang, N. Herron, V. V. Grushin, D. LeCloux, V. Petrov, *Appl. Phys. Lett.* **2001**, 79, 449.
- [16] T. Qin, J. Ding, L. Wang, M. Baumgarten, G. Zhou, K. Müllen, *J. Am. Chem. Soc.* **2009**, 131, 14329.
- [17] M. Sudhakar, P. I. Djurovich, T. E. Hogen-Esch, M. E. Thompson, *J. Am. Chem. Soc.* **2003**, 125, 7796.
-